Destructive and Nondestructive Evaluation of Corrosion of Reinforcing Bars in Concrete

C. Goksu[1], A. Ilki[2], and Y. Akkaya[2]

[1] PhD., Istanbul Technical University, Department of Civil Engineering, Istanbul, Turkey
[2] Prof., Istanbul Technical University, Department of Civil Engineering, Istanbul, Turkey

ABSTRACT: Corrosion, one of the most common durability problems in reinforced concrete structures, is an important factor in determination of the service life of the structures and assessment of performance against earthquakes. Therefore, detection of corrosion in structural members has received increasing attention in recent years, in order to take the necessary precautions and starting of the repair work in advance before the problem gets worse. In this paper, reinforced concrete columns with and without corrosion were examined by acoustic impact echo and electrochemical half-cell potential methods, and the results of these methods were evaluated together with visual inspection as well as seismic test results of these columns. It has been observed that, when these nondestructive methods are used in combination, it may be possible to detect the advancement of corrosion in reinforced concrete structures.

1   INTRODUCTION

Corrosion of reinforcement in concrete affects the load bearing capacity and the seismic behavior of structural components due to cross-section loss of reinforcing bar, cracking of cover concrete, loss of bond, and concentration of steel inelastic deformations at the mostly-pitted sections of reinforcing bars, especially during earthquakes. Thus, it is essential to identify the corrosion in order to heal the seismic performance of the structure. Although, corrosion is usually visually observable from the outside of the structural members due to cracks along the reinforcing bars and the change in the color of the concrete surface, it is essential to detect corrosion at least qualitatively before damage reaches a critical stage for the structure.

One of the nondestructive test methods to detect corrosion of the reinforcing bars is acoustic methods, such as impact-echo (IE), based on the use of impact-generated stress waves that propagate through the structure and are reflected by internal flaws, voids and cracks (Kim and Kim 2004). Electrochemical test methods, such as half-cell potential (HCP) and linear polarization (LP), are another type of test methods to detect corrosion potential and corrosion rate, respectively. HCP is based on the difference in electrochemical potential of active and passive reinforcing bars, while LP is based on the relationship between the electrochemical potential and the current generated between electrically charged electrodes and used in the calculation of the corrosion rate. The IE test method was used in the detection of reinforced concrete (RC) members by several researchers (Sansalone and Carino 1989, Lin and Sansalone 1992, Cheng and Sansalone 1993a, Cheng and Sansalone 1993b, Liang and Su 2001, Ozbora et. al. 2011). Moreover, Liang and Su (2001) used IE test method for detection of corrosion of reinforcing bars with lollipop concrete specimens.

In this study, RC columns were examined by using IE, HCP, and LP test methods both for uncorroded and corroded cases, and the results of these test methods were evaluated together with visual inspection as well as seismic loading test results of these columns.

2   SPECIMENS

The tests were carried out on 200×300×1390 mm (width×depth×height) RC columns, which were supported by a 700×700×500 mm (width×depth×height) footing. Clear concrete cover was 20 mm from the transverse bars. The reinforcement details of the specimens are shown in Figure 1a. The mean compressive strength of concrete at around testing dates is 25 MPa. Deformed 14 mm and 8 mm diameter bars were used as longitudinal and transverse reinforcing bars, respectively. The spacing of transverse bars is 100 mm.
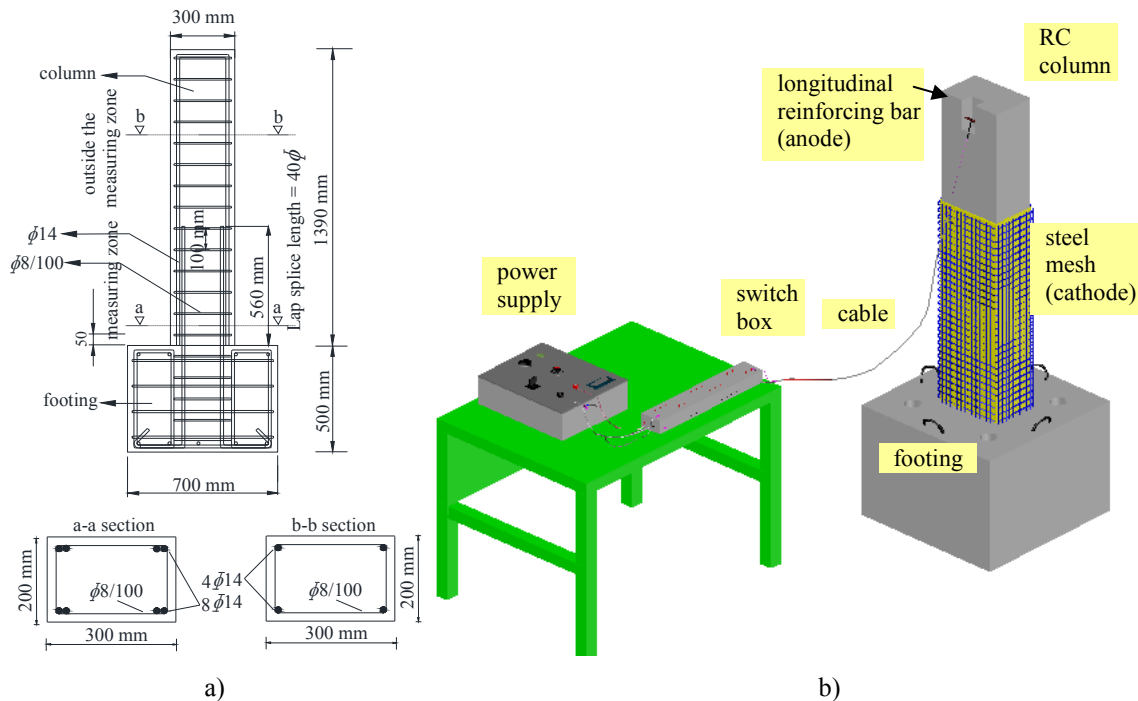

Figure 1. a) Reinforcement details of specimens, b) Accelerated corrosion setup

The bottom 900 mm height of the column specimens were subjected to accelerated corrosion process. For accelerated corrosion, calciumchloride ($CaCl_2$), 4% of the cement weight, was added into the mixing water of the concrete before casting. After casting, to increase the corrosion rate, $CaCl_2$ solution was sprayed to the outer sides of the columns and a fixed potential of 6 Volts was applied between steel mesh (cathode) and longitudinal reinforcement (anode) (Fig. 1b). The specimen denoted as Column-1, was not subjected to accelerated corrosion process, while the specimens Column-2, Column-3, Column-4 were subjected to similar accelerated corrosion process.

3   DETECTION OF CORROSION

3.1   *Visual observation*

Corrosion can generally be observed from the outside of the structural members due to cracks along the reinforcing bars and the change in the color of the concrete surface. An appearance of the column specimen after accelerated corrosion process is presented in Fig. 2a. After seismic test, the local losses in the cross-sections of reinforcing bars were determined by measuring the diameter of each 10 mm of reinforcing bar with a caliper in two directions (0º, 90º) after chemical cleaning of rust on reinforcing bars in accordance with ASTM G1 (2003). Then, some parts of reinforcing bars were scanned under 3D optical scanner (Fig. 2b-c). As seen in Fig. 2c, the pits due to corrosion, which caused up to 16% cross-section loss of reinforcing bar, can be clearly observed.

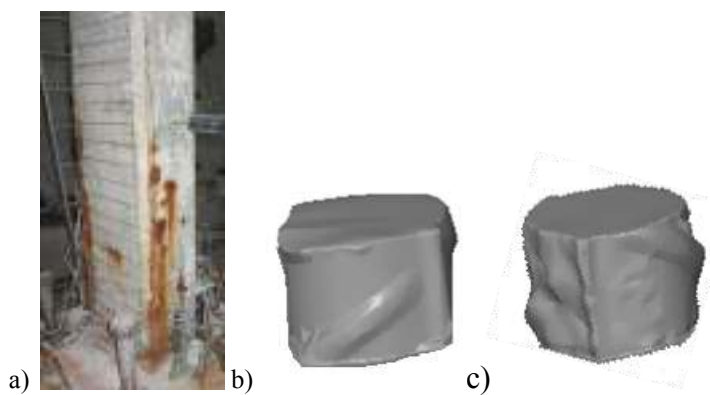a)   b)   c)

Figure 2. a) Appearance of a column specimen after accelerated corrosion process (before seismic test), the views of the b) Uncorroded, c) Corroded reinforcing bar obtained by the 3D optical scanner (after seismic test)

3.2   *Seismic test results*

The authors investigated the behavior of RC columns, which were subjected to various levels of reinforcement corrosion, in order to obtain the adverse effects of corrosion on the seismic performance of the columns and to evaluate the effect of corrosion on the damage mechanism (Goksu, 2012). Columns (Column-1, Column-2) were tested under reversed cyclic lateral and constant axial loads (20% of the axial load capacity of the tested columns). The test results of these columns (with and without corrosion) are presented in terms of load-displacement envelopes, energy dissipation capacities, and as well as strain distributions (Fig. 3a-c). In Fig. 3a, P is the applied lateral load and P_0 is the theoretical lateral load capacity of the specimens determined without considering the effect of corrosion. The horizontal load is corrected considering the horizontal component of the column axial load as suggested by PEER, Case I. The reductions in strength in Fig. 3a are because of the strength degradation of the specimens and the second order effects, which are not eliminated for the lateral load-drift ratio relationships of the column specimens. As seen in Fig. 3a, other than the significant decrease in the strength, the displacement capacity of the specimen Column-2, the specimen with corroded reinforcing bars, is also reduced due to concentration of plastic deformations of steel reinforcing bars at the pitted sections of the bar, preventing yielding of the bars outside the maximum pitted sections. Patch mortar, which was applied on Column-1 after casting due to defective workmanship, spalled prematurely during seismic test and caused the obligatory evaluation of the behaviors of the specimens in pushing direction only. In Fig. 3b, energy dissipations are calculated through the area enclosed by the hysteresis loops. As seen in Fig. 3b, the energy

dissipated by Column-2 is lower due to the reduced flexural strength and drift capacity, while Column-1, the specimen without corrosion, is able to dissipate much higher energy. The difference between the energy dissipation capacities stems from higher load resistance capacity of Column-1 even at larger drifts. The reinforcing bars of Column-1 and Column-2 ruptured at approximately 8% and 5% drift ratio, respectively. The premature rupture of the reinforcing bar of Column-2 can be attributed to corrosion, which prevented higher energy dissipation due to reduced lateral load capacity. Therefore, EDC-Drift ratio relationships for both columns are given until the drift ratio of 5%. However, Column-1 exhibited a more stable performance until 8% leading higher cumulative energy dissipation than shown in Fig. 3b. The variation of axial strains of starter bars of the Column-1 and Column-2 at different locations is presented in Fig. 3c. As seen in Fig. 3c, the starter bars of both columns yielded. However, the tensile strains, obtained from straingages, in the base of Column-1 were distributed and the strains at the same location were much smaller in Column-2 with corroded reinforcement.
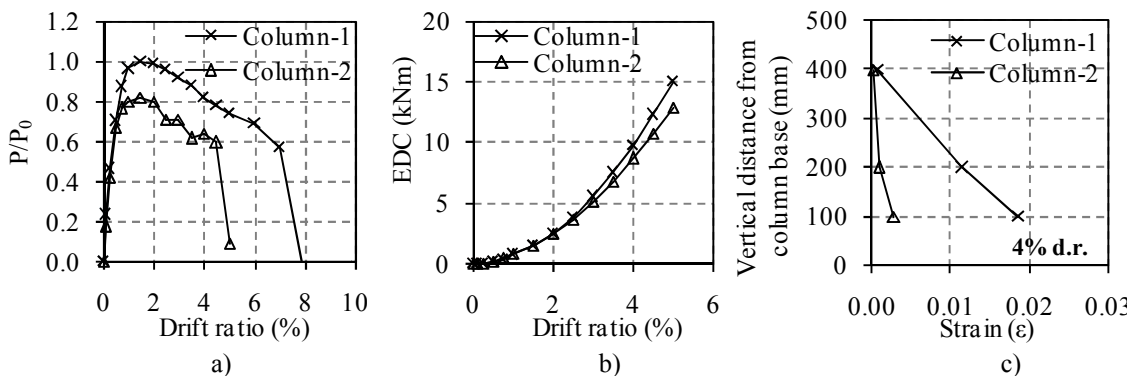

Figure 3. a) Envelope of load-displacement relationships, b) Energy dissipation capacities (EDC), c) Strain distribution (tensile strains while pushing) at 4% drift ratio (d.r.) of the columns

3.3 IE method

The IE method is an acoustic method, which is based on monitoring the surface motion resulting from a short-duration mechanical impact for the existence of any deterioration in concrete (Carino, 2001).
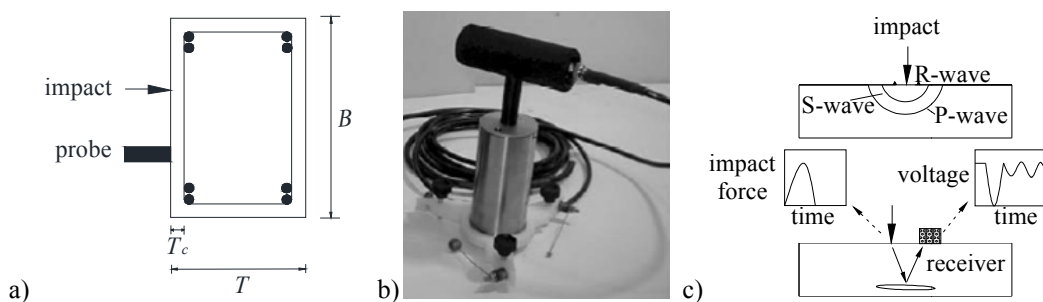

Figure 4. a) IE test set-up, b) Impactor steel balls wrapped around a receiver unit, c) The elastic stress wave signals generated by the IE method (Carino, 2001)

The IE test equipment is shown in Fig. 4a-c. The test equipment consists of an impactor (various sizes of steel balls) around a receiver probe, connected to a data acquisition system. Size of the steel ball determines the applied force and duration of the impact. Thus, when different sizes of steel balls are used as impactors, various frequencies of elastic stress waves can be generated.

These waves cause elastic displacements along their path, and when they meet with a transducer, the transducer translates this displacement information into voltage change vs. time.

Three types of waves are produced during an impact: R-, P- and S-waves. R-waves travel along the surface of the specimen, and thus, it is the first wave that is received by the transducer. R-waves can easily be detected as the first high energy peak in the voltage-time graph (Fig. 4c). P-waves are the compression waves that travel through the specimen and reflect back when an acoustically different material (such as cracks, voids, steel bars, specimen boundary) is hit. P-waves are faster and contain relatively higher energy, compared to shear waves (S-waves). P-waves bounce back and forth between the impact location and the acoustically different boundary, so they can also be easily detected by their periodic sine-wave like properties from the voltage-time graph (Fig. 4c). The estimation of the frequency range is the key point in corrosion detection for the IE method.

3.3.1 Estimation of the frequencies

The IE response of a rectangular column can be described by its aspect ratio, T/B. Here, T is the depth of the reflecting interface, and B is the perpendicular dimension of the member. At smaller aspect ratios, the element will behave like a plate, and for higher ratios the behavior will be more like a rod. The frequency for the first (fundamental) mode can be obtained by using Eq. 1, while the higher frequencies of the cross-sectional mode of vibrations can be obtained by a set of constants, characteristic to the geometry (T/B ratio) as described in Sansalone and Streett (1997). In Eq. 1, C_p is the P-wave speed through the thickness of the plate, which is 3250 m/s in this case, and β is a coefficient which depends on the ratio of T/B (Sansalone and Streett, 1997). In case there is a reinforcing bar in concrete, the frequency and the coefficient, ζ, can be obtained by using Eq. 2, and Eq. 3, respectively. In Eq. 3, R is the diameter of the transverse reinforcing bar (8 mm), and T_c is the distance from the transverse bar to the outside surface of the column. The parameters used in Eqs. 1-4, and the obtained frequencies are presented in Table 1.

As the lower parts (bottom 900 mm height of the column above the footing) of the columns were subjected to accelerated corrosion process, the measurements for the corroded cases were performed at these lower parts, while for the uncorroded case, measurements were performed at the upper parts (the rest 490 mm) of the column surfaces, at the level of the transverse reinforcing bars. The IE test results for the column specimens are presented in Tables 2. The P-wave speed in the columns was determined by the ultrasonic pulse velocity test. These frequencies are "expected frequencies" during the IE test of the RC columns.

$$f_1 = \beta C_p / 2T \tag{1}$$

$$f_{bar} = \zeta C_p / 4T_c \tag{2}$$

$$\zeta = \frac{-0.6R}{T_c} + 1.5 \, ; \, 0.3 < R/T_c < 0.83 \tag{3}$$
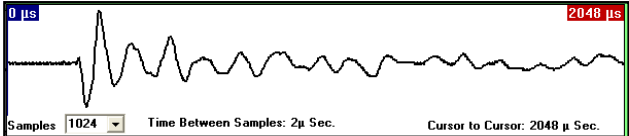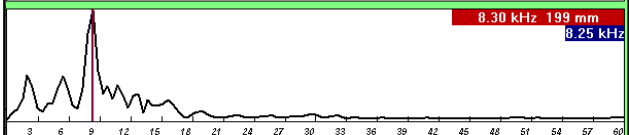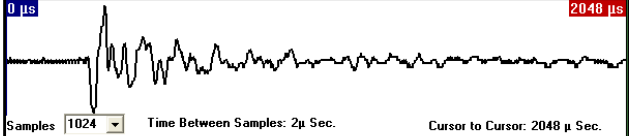
$$f_{cor} = \beta C_p / 2T_c \tag{4}$$
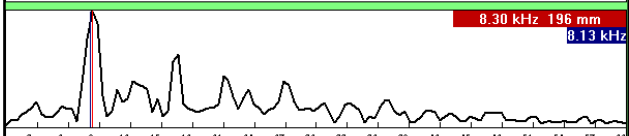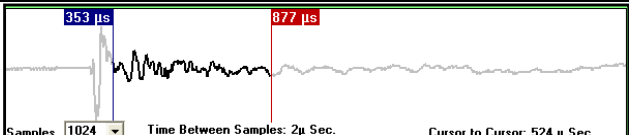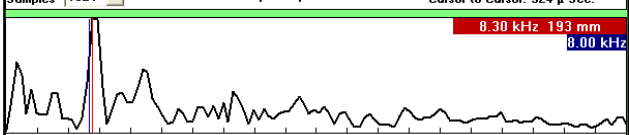
Table 1. The parameters used in the theoretical calculation of the frequencies

Specimen	T/B (mm/mm)	β	f_1 (kHz)	f_2 (kHz)	f_3 (kHz)	f_4 (kHz)	f_5 (kHz)	f_6 (kHz)	ζ	f_{bar} (kHz)	f_{cor} (kHz)
Column-2	200/300	0.85	6.9	7.7	10.3	10.7	13.2	13.5	1.3	44.0	57.5
Column-3,4	300/200	0.94	5.1	8.0	10.4	11.0	13.2	13.6	1.3	44.0	57.5

3.3.2 IE test results of the specimens

Table 2 presents the voltage-time, and frequency-amplitude graphs for corroded and non-corroded columns. During the IE test, the voltage changes, caused when surface and reflected stress waves were received by the receiver probe, were recorded in time domain. Then, the waveforms in time domain were converted to frequency domain by applying Fast-Fourier transformation, to determine the dominant frequency. As seen from Table 2a, tapping with a 12 mm diameter steel ball, the frequency of the reinforcing bar could not be obtained due to the long-duration impact. This is because the wave length of the generated stress wave is larger than the reinforcing bar diameter. As seen from Table 2a, the fundamental frequency is 8.3 kHz (By default, β was taken as 0.94, as for plate-like structures). If the β value is taken as 0.85 as a surrogate for 0.94 in this case, the fundamental frequency would be 7.6 kHz, which is very close to the estimated frequency, 6.9 kHz. As seen from Table 2a, the cross-sectional mode frequencies are at about 8, 10, 13 kHz, which are also very close to the other estimated mode frequencies.

Table 2. Sample IE test results of the specimens

Corrosion status	x - y axis	Spectrums
a Non-corroded case, 12 mm diameter ball	$V(volt)$ - t(μs) A - $f(kHz)$	
b Non-corroded case, 4 mm diameter ball	$V(volt)$ - t(μs) A - $f(kHz)$	
c Corroded case, 4 mm diameter ball	$V(volt)$ - t(μs) A - $f(kHz)$	

As seen from Table 2b, tapping with a 4 mm diameter steel ball, the frequency of the reinforcing bar could be obtained clearly due to smaller diameter of the ball. Among the measured values, there are frequencies, which are very close to f_{bar}. Frequency of the corroded section of the column, T_c should be taken as 24 mm since the stress waves can travel only along the concrete cover. The reinforcing bars on the opposite side of the column (T_c=176 or 276 mm)

can be ignored, since R/T_c is smaller than 0.3 according to Eq. 3. Flexural frequency at about 1 kHz can be attributed to corrosion, resulting from shallow cracks (Table 2c). The corrosion frequency can be observed in Table 2c.

3.4 Electrochemical test methods

For the measurement of corrosion potential through HCP method and corrosion rate through LP method of the column specimens, a portable corrosion meter, GECOR8, was used (Figure 5). The measurements were performed at certain time intervals on the specimen Column-1 for uncorroded case, and on the specimens Column-2, Column-3, Column-4 for corroded cases.

Figure 5. Corrosionmeter test set-up

3.4.1 HCP test method and results

The corrosion potential (E_{corr}) is the indicative of the probability of corrosion activity of the reinforcing bar. According to ASTM C876 (1999), the corrosion potential more than -200 mV, between -200 and -350 mV, between -350 and -500 mV and less than -500 mV corresponds to low corrosion risk (%10 probability), medium corrosion risk (%50 probability), high corrosion risk (%90 probability) and severe corrosion risk, respectively. The principle of the equipment is based on measuring a potential difference against a reference electrode, which is $Cu/CuSO_4$ in this case (Elsener et al. 2003). As seen from Figure 6a, as Column-1 is the specimen without corrosion, the corrosion potential is more than -200 mV, and the specimens with corroded reinforcing bars (Column-2, Column-3, Column-4) have corrosion potential of less than -500 mV, and the corrosion potential decreases in a regular trend by the increase of corrosion activity. At the initial stage of the monitoring process, the corrosion potential of Column-2, Column-3, Column-4 is less than their values at further stages, as in the studies of Nakamura et al. (2008) and Andrade et al. (2002), which can be attributed to daily weather changes.

3.4.2 LP test method and results

LP test method allows the user to obtain quantitative information on the deterioration rate (Broomfield et al. 1994). However, as seen in Figure 6b, there is no precise trend by means of corrosion rate (I_{corr}) in this study as in the study of Andrade et al. (2002). This behavior can be attributed to the environmental factors, such as daily changes in temperature and water saturation. It was expected to observe that the specimens would behave as noncorroding ($I_{corr} \approx 0.1$) at the beginning of the monitoring process and corroding ($0.5 \leq I_{corr} \leq 1$) by time, in accordance with visual observations from outside.
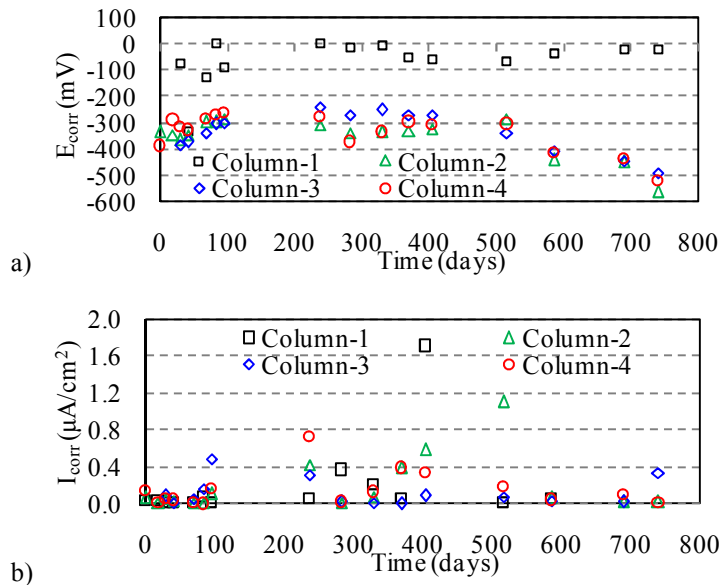
Figure 6 a) HCP, b) LP test results of the column specimens

Nondestructive methods, such as IE (based on acoustic principles), and semi-destructive methods, such as HCP (based on electrochemical principles) measurements have the potential of indicating the corrosion of the reinforcing bars in a RC member, while another semi-destructive method LP did not show consistency with the other evaluations considered in this study. In order to evaluate the peaks and frequencies of the IE test results, expected frequencies of the structural member, based on its geometry and dimensions, should be calculated in advance. Due to variation in test results and effect of possible environmental factors, IE and HCP test methods can be used in complement with each other. IE test method can be performed on many locations, where HCP and LP measurement locations are limited.

4   CONCLUSIONS

In this study, four cantilever RC columns were constructed for representing the columns of ordinary structures complying with the regulations of recent seismic design codes. The specimens, except the reference one, were subjected to accelerated corrosion process. The corrosion activity is reported in terms of visual observations, seismic loading test, acoustic and electrochemical methods.

- Corrosion caused cracking along the reinforcing bars, change in the color of the concrete surface as well as localized attacks (pits) on the cross-section of the reinforcing bars,

- The pits can lead to reduced displacement capacity for the columns with corroded reinforcing bars due to concentration of plastic deformations of main reinforcing bars at and around the maximum cross-section loss zone,

- When used together, nondestructive and semi-destructive methods have the potential of indicating the corrosion activity of the RC members.

5   ACKNOWLEDGEMENTS

6   REFERENCES

ASTM G1. 2003. Standard practice for preparing, cleaning and evaluating corrosion test specimens. *The American Society for Testing and Materials*, Pennsylvania.

ASTM C876.1999. Standard test method for half-cell potentials of uncoated reinforcing steel in concrete. *The American Society for Testing and Materials*, Pennsylvania.

Andrade, C, Alonso, C, Sarria, J. 2002. Corrosion rate evolution in concrete structures exposed to the atmosphere. *Cement and Concrete Composites*, 24: 55-64.

Broomfield JP, Rodriguez, J, Ortega, LM, Garcia AM. 1994. Corrosion rate measurements in reinforced concrete structures by a linear polarization device. *ACI Special Publication*, 151:163-182.

Carino, NJ. 2001. The impact-echo method: an overview. *Proceedings of the 2001 Structures Congress & Exposition*, Washington, US. Virginia: Chang, PC.

Cheng, C, and Sansalone, M. 1993a. The impact-echo response of concrete plates containing delaminations: numerical, experimental and field studies. *Materials and Structures*, 26(159): 274-285.

Cheng, C, and Sansalone, M. 1993b. Effects on impact-echo signals caused by steel reinforcing bars and voids around bars. *ACI Materials Journal*, 90 (5): 421-434.

Elsener, B, Andrade, C, Guliker, J, Polder, R. 2003. Half-cell potential measurements-potential mapping on reinforced concrete structures. *Material and Structures*, 36:461-471.

Goksu, C. 2012. Seismic behavior of RC columns with corroded plain and deformed reinforcing bars. *PhD Thesis*, Istanbul Technical University, Istanbul, Turkey.

Kim, DS, and Kim, HW. 2004. Non-destructive testing and evaluation of civil infrastructures using stress wave propagation. *Key Engineering Materials*, 270-273: 1616-1621.

Liang, MT, and Su, PJ. 2001. Detection of the corrosion damage of rebar in concrete using impact-echo method. *Cement and Concrete Research,* 31: 1427-1436.

Lin, Y, and Sansalone, M. 1992. Detecting flaws in concrete beams and columns using the impact-echo method. *ACI Materials Journal*, 89(4): 394-405.

Nakamura E, Watanabe H, Koga H, Nakamura M, and Ikawa K. 2008. Half-cell potential measurements to assess corrosion risk of reinforcement steels in a PC bridge. *International RILEM Conference on Site Assessment of Concrete, Masonry and Timber SACOMATIS 2008*, Italy.

Ozbora AA, Basar NU, Akkaya Y, and Tasdemir MA. 2011. Use of NDT in Condition Assessment. *Nondestructive Testing of Materials and Structures NDTMS 2011*, Turkey.

PEER Structural and Performance Database. 2004. University of California, Berkley, USA.

Sansalone, M, and Carino, NJ. 1989. Detecting delaminations in concrete slabs with and without overlays using the impact-echo method. *Journal of the American Concrete Institute*, 86 (2): 175-184.

Sansalone, M, and Streett, WB. 1997. Impact-echo: Nondestructive testing of concrete and masonry. Bullbrier Press, Jersey Shore, PA.